

SRC TR 87-186

**Structured Singular Value and  
Geometry of the m-Form Numerical  
Range**

**by**

**J. Wang, M.K.H. Fan, and A.L. Tits**

# Structured Singular Value and Geometry of the $m$ -Form Numerical Range \*

Jia-Chang Wang      Michael K.H. Fan      André L. Tits <sup>†</sup>

Electrical Engineering Department and Systems Research Center

University of Maryland, College Park, MD 20742

September 16, 1987

## Abstract

Although the question of the numerical evaluation of Doyle's structured singular value has been repeatedly addressed, it is not yet entirely resolved in the case of block structures of size larger than 3. It has been shown recently that this question can be reduced to that of iteratively computing the distance from the origin to the  $m$ -form numerical range of certain tuples of matrices. How to effectively compute such distances in the nonconvex case (which may arise when dealing with more than 3 blocks) is an open problem. In this paper, in an attempt to tackle this problem, the question of graphically displaying sections of the  $m$ -form numerical range is investigated.

## 1 Introduction

The concept of structured singular value was introduced by Doyle [1] as a tool for the analysis and synthesis of feedback systems affected by structured uncertainties. It is a key to the design of control systems under joint robustness and performance specifications and it nicely complements the  $H^\infty$  approach to control system design [2,3]. It has already been used successfully in various application areas [4-7]. The question of how to numerically evaluate, in a reliable manner, the structured singular value of a matrix has been explored by several authors [1,8-11] but is not entirely resolved yet.

---

\*This research was supported by the National Science Foundation under grants No. DMC-84-51515 and CDR-85-00108.

<sup>†</sup>Please address all correspondence to the third author.

Given an  $m$ -tuple  $\mathcal{K} = (k_1, \dots, k_m)$  of positive integers, referred to as *block-structure* of size  $m$ , the structured singular value  $\mu$  of a square complex matrix  $M$  of size  $n = \sum_{i=1}^m k_i$  can be defined as (see [9,12])<sup>1</sup>

$$\mu = \max_{x \in \mathbb{C}^n} \{ \|Mx\| : \|P_i x\| \|Mx\| = \|P_i Mx\|, i = 1, \dots, m \} . \quad (1)$$

where, for  $i = 1, \dots, m$ ,

$$P_i = \text{block diag } (O_{k_1}, \dots, O_{k_{i-1}}, I_{k_i}, O_{k_{i+1}}, \dots, O_{k_m}) ,$$

where, for any positive integer  $k$ ,  $I_k$  is the  $k \times k$  identity matrix and  $O_k$  the  $k \times k$  zero matrix and where  $\|\cdot\|$  denotes the Euclidean norm. The question of efficiently computing  $\mu$  has been resolved for the case when  $m \leq 3$  [1,9] but is still open in the general case. In particular, formula (1) is of limited help as the optimization problem it involves generally has some nonglobal maximizers. Also, if  $m \leq 3$ , the structured singular value can be obtained by solving the quasi-convex problem

$$\mu = \inf_{D \in \mathcal{D}} \bar{\sigma}(DMD^{-1}) \quad (m \leq 3) \quad (2)$$

where

$$\mathcal{D} = \{ \text{block diag } (d_1 I_{k_1}, \dots, d_m I_{k_m}) : d_i \in (0, \infty) \}$$

and where  $\bar{\sigma}$  indicates the largest singular value. While (2) often holds when  $m > 3$ , its right hand side is sometimes a strict upper bound to  $\mu$ , as is the case in an example suggested by Doyle[13](see Appendix) hereafter referred to as Example D. In [10] it is shown that the concept of structured singular value is related to that of  $m$ -form numerical range of certain tuples of matrices. The  *$m$ -form numerical range* of an  $m$ -tuple of  $n \times n$  Hermitian matrices  $A_1, \dots, A_m$  is the set

$$W(A_1, \dots, A_m) = \{ f(x) : x \in \partial B \}$$

where  $\partial B$  is the unit sphere in  $\mathbb{C}^n$ , i.e.,

$$\partial B = \{ \|x\| = 1, x \in \mathbb{C}^n \} ,$$

where  $f: \mathbb{C}^n \rightarrow \mathbb{R}^m$  has components

$$f^i(x) = x^H A_i x, i = 1, \dots, m.$$

---

<sup>1</sup>This definition of the structured singular value, while computationally more tractable, is equivalent to that originally proposed by Doyle [1]:  $\mu_{\mathcal{K}}(M) = 0$  if there is no block diagonal matrix  $\Delta$ , with  $i$ th block of size  $k_i$ , such that  $\det(I + M\Delta) = 0$ ;  $\mu_{\mathcal{K}}(M) = (\min\{\bar{\sigma}(\Delta) : \det(I + M\Delta) = 0\})^{-1}$  otherwise, where the 'min' is taken over the same family of block diagonal matrices.

It is shown in [10] that, if one defines, for  $\alpha \in \mathbb{R}$ ,

$$A_i(\alpha) = \alpha P_i - M^H P_i M$$

where the superscript ‘ $H$ ’ indicates the complex conjugate transpose, and if one denotes by  $W(\alpha)$  the  $m$ -form numerical range  $W(A_1(\alpha), \dots, A_m(\alpha))$ , the structured singular value of  $M$  is given by

$$\mu = \lim_{k \rightarrow \infty} \sqrt{\alpha_k}$$

where  $\alpha_k$  is recursively defined by

$$\begin{aligned} \alpha_0 &= \bar{\sigma}^2(M) = \max_{\|x\|=1} \|Mx\|^2 \\ \alpha_{k+1} &= \alpha_k - c(\alpha_k), \quad k = 0, 1, 2, \dots \end{aligned}$$

with

$$c(\alpha) = \min\{\|v\| : v \in W(\alpha)\}.$$

Thus the question of computing  $\mu$  is reduced to that of iteratively computing the distance  $c(\alpha_k)$  from the origin to the  $m$ -form numerical range  $W(\alpha_k)$ .

In this paper, in an attempt to address the latter question, we examine properties of  $W(\alpha)$  and propose procedures to graphically display the boundaries of its 2-dimensional sections. In Section 2, some properties of the  $m$ -form numerical range are reviewed. In Sections 3 and 4 the question of graphically displaying 2-dimensional sections of the  $m$ -form numerical range is investigated. In Section 3 it is shown that if one rotates and translates the  $m$ -form numerical range so as to map any given  $k$ -dimensional section to the subspace spanned by the last  $k$  coordinate axes, the resulting set is still an  $m$ -form numerical range; thus there is no loss of generality in considering only sections of the latter type. In Section 4, procedures are proposed to display (or attempt to display) 2-dimensional such sections. Several examples are considered, including Example D.

## 2 Some Properties of the Generalized Numerical Range

Given  $m$  complex Hermitian  $n \times n$  matrices  $A_1, \dots, A_m$ , their  $m$ -form numerical range  $W = W(A_1, \dots, A_m)$  satisfies the following properties.

**Property 1.**[14–17]<sup>2</sup> If  $n = 2$  and  $m = 3$ ,  $W$  is (the boundary of) an ellipsoid. In all other cases, if  $m \leq 3$ ,  $W$  is convex. If the  $A_i$ ’s are real symmetric then, if  $m \leq 3$ ,  $W$  is always convex.  $\square$

---

<sup>2</sup>For  $m = 2$ , this result has been long known [18,19].

Note that, in our context, the first alternative cannot occur since  $n \geq m$ .

**Property 2.**[17]The intersection of  $W(A_1, \dots, A_m)$  with any of its supporting hyperplanes is an  $\mathbb{R}^m$ -imbedding of the  $m$ -form numerical range of a certain  $(m - 1)$ -tuple of matrices.  $\square$

The next property is an immediate consequence of Properties 1 and 2.

**Property 3.** If  $m = 4$  and  $A_1, \dots, A_4$  are real symmetric, then  $W$  has a convex boundary, i.e., the intersection of  $W$  with any of its supporting hyperplanes is convex.  $\square$

**Property 4.**[17]If  $x \in \partial B$  is such that  $f(x)$  is on the boundary of  $W(A_1, \dots, A_m)$  then there exists a direction  $w \in \mathbb{R}^m$  such that  $x$  is an eigenvector of  $\sum_{k=1}^m w^k A_k$ . Moreover (i) if  $\mathcal{H}$  is any supporting hyperplane to  $W(A_1, \dots, A_m)$  at  $f(x)$ , then the direction orthogonal to  $\mathcal{H}$  is a valid choice for  $w$ . if (ii) for some  $q \in \{1, \dots, m - 1\}$  there exists no subset of  $W(A_1, \dots, A_m)$  containing  $f(x)$  that is locally homeomorphic to  $\mathbb{R}^{m-q}$  around  $f(x)$ , then there is a  $(q + 1)$ -dimensional subspace  $S$  of  $\mathcal{V} = \{A \in \mathbb{C}^{n \times n} : A = \sum_{k=1}^m w^k A_k, w^i \in \mathbb{R}\}$  such that all matrices in  $S$  admit  $x$  as an eigenvector.  $\square$

With  $W(\alpha)$  as defined in Section 1, the following holds.

**Property 5.**[10]

$$\mu = \inf_{D \in \mathcal{D}} \bar{\sigma}(DMD^{-1}) \quad (3)$$

if, and only if there exists a vector  $\lambda \in \mathbb{R}^m$ , with  $\lambda^i \geq 0$  for all  $i$ , such that  $W(\mu^2)$  is contained in the closed half space

$$H(\lambda) = \{v \in \mathbb{R}^m | \langle v, \lambda \rangle \geq 0\} . \quad \square$$

We conclude this section with two conjectures.

**Conjecture 1.** For complex  $A_1, \dots, A_m$ , if  $m \leq 2n - 2$  and  $W$  has a convex boundary, then  $W$  is convex.  $\square$

**Conjecture 2.** For any  $m$ , if  $A_1, \dots, A_m$  are real symmetric,  $W$  has a convex boundary.  $\square$

### 3 Coordinate Transformations

In this section, we show that if one rotates and translates an  $m$ -form numerical range so as to map any given  $k$ -dimensional section to the subspace spanned by the last  $k$  coordinate axes, the resulting set is still an  $m$ -form numerical range.

The intersection, denoted by  $\Lambda$ , of the  $m$ -form numerical range  $W$  of matrices  $A_1, \dots, A_m$  with a  $k$ -dimension affine space can be expressed as

$$\Lambda = W \cap H_1 \cap \dots \cap H_{m-k}$$

where, for  $i = 1, \dots, m - k$ ,  $H_i$  is the one-dimensional hyperplane defined as

$$H_i = \{v \in \mathbb{R}^m \mid \langle v, u_i \rangle = \lambda^i\}$$

for some  $u_i \in \mathbb{R}^m$ ,  $\lambda^i \in \mathbb{R}$ . Without loss of generality, it can be assumed that the  $u_i$ 's are orthonormal.

Now consider the following coordinates transformation

$$\hat{v} = U^T v - \lambda \quad (\text{or } v = U(\hat{v} + \lambda)) \quad (4)$$

where

$$U = [u_1 \dots u_m]$$

for some  $u_{m-k+1}, \dots, u_m$ , such that  $U$  is an orthonormal matrix (i.e.,  $U^T U = I$ ), and

$$\lambda = [\lambda^1 \dots \lambda^m]^T$$

with arbitrary  $\lambda^{m-k+1}, \dots, \lambda^m$ . Transformation (4) is a composition of coordinates rotation and translation. Under this transformation, it is easily checked that the image of the  $k$ -dimension section  $\hat{\Lambda}$  of the  $m$ -form numerical range is

$$\hat{\Lambda} = \hat{W} \cap \hat{H}_1 \cap \dots \cap \hat{H}_{m-k} \quad (5)$$

where  $\hat{W}$  is the image of  $W$  and similarly for  $\hat{H}_i$ ,  $i = 1, \dots, m - k$ . Since

$$W = \{v \in \mathbb{R}^m : \exists x \in \partial B \text{ s.t. } v^i = x^H A_i x \forall i \in \{1, \dots, m\}\},$$

we obtain

$$\begin{aligned} \hat{W} &= \{\hat{v} \in \mathbb{R}^m : \exists x \in \partial B \text{ s.t. } \hat{v} = U^T v - \lambda, \text{ with } v^i = x^H A_i x \forall i \in \{1, \dots, m\}\} \\ &= \{\hat{v} \in \mathbb{R}^m : \exists x \in \partial B \text{ s.t. } \hat{v}^i = x^H \hat{A}_i x \forall i \in \{1, \dots, m\}\} \\ &= W(\hat{A}_1, \dots, \hat{A}_m) \end{aligned} \quad (6)$$

where, for  $i = 1, \dots, m$ ,

$$\hat{A}_i = \sum_{j=1}^m U_{ji} A_j - \lambda^i.$$

Similarly, for  $i = 1, \dots, m - k$ ,

$$\begin{aligned} \hat{H}_i &= \{\hat{v} \in \mathbb{R}^m \mid \hat{v} = U^T v - \lambda, \langle v, u_i \rangle = \lambda^i\} \\ &= \{\hat{v} \in \mathbb{R}^m \mid \langle U(\hat{v} + \lambda), u_i \rangle = \lambda^i\} \\ &= \{\hat{v} \in \mathbb{R}^m \mid \hat{v}^i = 0\} \end{aligned} \quad (7)$$

Since  $U$  is orthonormal, it follows from (4), (5), (6) and (7) that  $\Lambda$  can be obtained by translation and rotation from the intersection of the  $m$ -form numerical range of  $\hat{A}_1, \dots, \hat{A}_m$  with the span of the last  $k$  coordinate axes.

## 4 Graphically Displaying $W$

In the 2-dimensional case ( $m = 2$ ), the following simple procedure displays the boundary of  $W$  (see [10,12]).

### Procedure 1.

*Step 0.* Set  $\theta = 0$  and  $N =$  a large integer.

*Step 1.* Let  $x$  be any unit length eigenvector corresponding to the smallest eigenvalue of  $\cos \theta A_1 + \sin \theta A_2$ . Set

$$y_2 = \begin{bmatrix} x^H A_1 x \\ x^H A_2 x \end{bmatrix}$$

If  $\theta \neq 0$ , draw the line segment  $\overline{y_1 y_2}$ . If  $\theta \geq 2\pi$ , stop.

*Step 2.* Set  $y_1 = y_2$ ,  $\theta = \theta + 2\pi/N$  and go to Step 1.  $\square$

Figure 1 depicts  $W(A_1, A_2)$  with

$$A_1 = \begin{bmatrix} 1 & 0 & 0 \\ 0 & -1 & 1 \\ 0 & 1 & -1 \end{bmatrix} \quad A_2 = j \begin{bmatrix} 0 & 0 & 0 \\ 0 & 0 & -1 \\ 0 & 1 & 0 \end{bmatrix}$$

where  $j = \sqrt{-1}$  (the example is borrowed from [21] where a different algorithm is used to plot  $W$ ). In agreement with Property 4, the point  $(1, 0)$  is the image of an eigenvector  $[1, 0, 0]^T$  of all linear combinations of  $A_1$  and  $A_2$ , i.e., an eigenvector of both  $A_1$  and  $A_2$ .

Consider now the question of displaying convex 2-dimensional sections of  $W$ . In view of the discussion in Section 3, without loss of generality, suppose that the section of interest is defined by  $w_i = 0$ ,  $i = 1, \dots, m - 2$ . The following procedure is suggested.

### Procedure 2.

*Step 0.* Set  $\theta = 0$  and  $N =$  a large integer.

*Step 1.* Find  $z_3, \dots, z_m$  (e.g. using a Newton iteration) such that, for  $i = 1, \dots, m-2$ ,  $x^H A_i x = 0$  where  $x$  is any unit length eigenvector corresponding to the smallest eigenvalue of  $\cos \theta A_1 + \sin \theta A_2 + \sum_{i=3}^m z_i A_i$ . Set

$$y_2 = \begin{bmatrix} x^H A_1 x \\ x^H A_2 x \end{bmatrix}$$

If  $\theta \neq 0$ , draw the line segment  $\overline{y_1 y_2}$ . If  $\theta \geq 2\pi$ , stop.

*Step 2.* Set  $y_1 = y_2$ ,  $\theta = \theta + 2\pi/N$  and go to Step 1.  $\square$

In view of Properties 1 and 3, Procedure 2 will correctly display the boundary of  $W$  when  $m = 3$  and the ‘outer’ boundary of  $W$  when  $m = 4$  and the  $A_i$ ’s are real. It should be clear that, if the section under consideration is not convex, Procedure 2 will display the *convex hull* of its boundary. Figure 2 was generated by Procedure 2. It is the section by a 2-dimensional affine space passing through the origin of the convex hull of the  $m$ -form numerical range  $W(\mu^2)$  ( $\mu \approx .87$ ) corresponding to Example D (see Appendix). As a side point, notice that on both Figures 1 and 2, Procedures 1 and 2 naturally space points  $y_i$  proportionally to the curvature (this property can be easily proved). Thus more points are used in region of high curvature, as is desirable. This property is illustrated on Figure 3.

Our main purpose in this paper is to investigate the geometric properties of  $W$  in the non-convex case. Thus we turn now to the question of graphically displaying nonconvex 2-dimensional sections of  $W$ . The next procedure uses ‘brute force’ to display the intersection of any given  $W$  with the span of the last two coordinate axes.

### Procedure 3.

*Step 1.* Randomly generate  $x_i \in \mathbb{C}^n$ ,  $x_i \neq 0$ ,  $i = 1, \dots, m-1$ .

*Step 2.* Find  $\beta_i$ ,  $i = 1, \dots, m-2$  such that, for  $j = 1, \dots, m-2$ ,

$$\left( \sum_{i=1}^{m-2} \beta_i x_i + x_{m-1} \right)^H A_j \left( \sum_{i=1}^{m-2} \beta_i x_i + x_{m-1} \right) = 0$$

*Step 3.* Set  $x = \sum_{i=1}^{m-2} \beta_i x_i + x_{m-1}$ . If  $x = 0$ , go to Step 1. Else set  $x = x/\|x\|$  and

$$y = \begin{bmatrix} x^H A_1 x \\ x^H A_2 x \end{bmatrix}$$

Draw a small dot at  $y$ . Go to Step 1.  $\square$



In view of Property 5, Example D (see Appendix) corresponds to a set  $W(\mu^2)$  for which there is no  $\lambda \geq 0$  such that  $W(\mu^2)$  is contained in the closed half space  $\{v \in \mathbb{R}^4 \mid \langle v, \lambda \rangle \geq 0\}$ . Figure 4 (generated using Procedure 3), which displays that intersection of  $W(\mu^2)$  with a 2-dimensional affine set passing through the origin, illustrates this point. The ‘corner’ at 0 on the same picture indicates, in view of Property 4 (ii), that 0 is the image under  $f$  of a vector  $x \in \mathbb{R}^n$  which is an eigenvalue of all matrices in a 2-dimensional subspace of the real span of the  $A_i$ ’s.

Clearly Procedure 3 is computationally expensive. As an alternative, one can try to make use of Property 4. This possibility was investigated in the particular case of Example D. Figure 5 shows the boundary of the section displayed on Figure 4. The ‘convex’ portion of this boundary was drawn using Procedure 2. It turns out that, in this case, the ‘nonconvex’ portion is constituted of images of eigenvectors corresponding to the *second* largest eigenvalue of the linear combination  $\sum_i w_i A_i$ , with  $w$  a vector orthogonal to the hyperplane ‘tangent to  $W(\mu^2)$ ’ at the point under consideration. A similar technique was used to generate Figures 6 to 9. These also come from Example D, this time with  $\alpha = 1$ . As seen on Figure 6,  $\text{co}W(1)$  touches the origin (while  $W(1)$  does not) and the corresponding supporting hyperplane  $H$  intersects  $W(1)$  at more than one point. Clearly, the ‘contact surface’ is not convex so that, in view of Properties 1 and 2, it must be an ellipsoid. This is confirmed by Figures 7 to 9 which depict 2-dimensional sections contained in 3-dimensional sections of  $W$  defined by hyperplanes parallel to  $H$ .

## 5 Appendix: Example D

For easy of reference, we reproduce here an example due to Doyle [13] where  $m = 4$  and equality in (2) does not hold. Some background from [1] is given first.

For a complex  $n \times n$  matrix  $M$ , consider the singular value decomposition

$$M = [U_1 \ U_2] \Sigma [V_1 \ V_2]^H ,$$

where  $U_1, V_1 \in \mathbb{C}^{n \times r}$  with  $r$  the multiplicity of  $\bar{\sigma}(M)$  and  $[U_1 \ U_2], [V_1 \ V_2]$  are unitary. Define

$$\nabla_2 = \{z \in \mathbb{R}^{m-1} : \exists v \in \mathbb{C}^r, \|v\| = 1 \text{ s.t. } z_i = v^H H_i v, \forall i \in \{1, \dots, m-1\}\}$$

where

$$H_i = \frac{1}{2}(U_1^H M_i V_1 + V_1^H M_i^H U_1)$$

and

$$M_i = P_i M - M P_i .$$

The following two facts are proved in [1].

**Fact 1.**  $\inf_{D \in \mathcal{D}} \bar{\sigma}(DMD^{-1}) = \bar{\sigma}(M)$  if, and only if,  $0 \in \text{co}\nabla_2$ .  $\square$

**Fact 2.**  $\mu(M) = \bar{\sigma}(M)$  if, and only if,  $0 \in \nabla_2$ .  $\square$

Doyle's example is as follows. Let

$$M = \begin{bmatrix} a & 0 \\ ab & ab \\ ab & abj \\ \sqrt{1-2a^2} & \frac{-a^2(1+j)}{2\sqrt{1-2a^2}} \end{bmatrix} \begin{bmatrix} 0 & a \\ ab & -ab \\ ab & -abj \\ \frac{a^2(1-j)}{2\sqrt{1-2a^2}} & \sqrt{1-2a^2} \end{bmatrix}^H$$

and

$$\mathcal{K} = (1, 1, 1, 1)$$

where  $a = \sqrt{1 - \frac{\sqrt{3}}{3}}$ ,  $b = \frac{\sqrt{2}}{2}$  and  $j = \sqrt{-1}$ . One obtains

$$H_1 = a^2 \begin{bmatrix} 1 & 0 \\ 0 & -1 \end{bmatrix}, \quad H_2 = a^2 \begin{bmatrix} 0 & 1 \\ 1 & 0 \end{bmatrix}, \quad H_3 = a^2 \begin{bmatrix} 0 & j \\ -j & 0 \end{bmatrix}$$

and it is easy to check that  $\nabla_2$  is a circle with radius  $a^2$  centered at the origin. Thus, by Facts 1 and 2, we have

$$\inf_{D \in \mathcal{D}} \bar{\sigma}(DMD^{-1}) = \bar{\sigma}(M) \neq \mu(M).$$

## References

- [1] J.C. Doyle, "Analysis of Feedback Systems with Structured Uncertainties," *Proc. IEE-D* 129 (1982), 242–250.
- [2] J.C. Doyle, "Structured Uncertainty in Control System Design," *Proceedings of the 24th IEEE Conference on Decision and Control*, Fort Lauderdale, Florida (December 1985).
- [3] M.G. Safonov, "Optimal H-infinity Synthesis of Robust Controller for Systems with Structured Uncertainty," *Proceeding of the 25th IEEE Conference on Decision and Control*, Athens, Greece (December 1986).
- [4] J.C. Doyle, K. Lenz & A. Packard, "Design Examples Using Mu-Synthesis: Space Shuttle Lateral Axis FCS During Reentry," *Proceeding of the 25th IEEE Conference on Decision and Control*, Athens, Greece (December 1986).
- [5] G.J. Balas & J.C. Doyle, "Feedback Design for a Large Space Structure Experiment," *Proc. of the 10th IFAC World Congress 8* (July 1987), 426–429.
- [6] S. Skogestad & M. Morari, "Robust Control of Distillation Columns," *Proc. of the 10th IFAC World Congress 2* (July 1987), 281–286.
- [7] E. Zafiriou & M. Morari, "Robust  $H_2$ -Type IMC Controller Design Via the Structured Singular Value," *Proc. of the 10th IFAC World Congress 2* (July 1987), 275–280.
- [8] B. Kouvaritakis & H. Latchman, "Necessary and Sufficient Stability Criterion for Systems with Structured Uncertainties: the Major Principal Direction Alignment Principle," *Internat. J. Control* 42 (1985), 575–598.
- [9] M.K.H. Fan & A.L. Tits, "Characterization and Efficient Computation of the Structured Singular Value," *IEEE Trans. Automat. Control* AC-31 (1986), 734–743.
- [10] M.K.H. Fan & A.L. Tits, " $m$ -Form Numerical Range and the Computation of the Structured Singular Value," *IEEE Trans. Automat. Control* (1987), to appear.
- [11] J.W. Helton, "A Numerical Method for Computing the Structured Singular Value," University of California, San Diego, Technical Report, 1987.
- [12] M.K.H. Fan, "Characterization and Computation of the Structured Singular Value," University of Maryland, PhD Thesis, College Park, MD 20742, 1986.
- [13] J.C. Doyle, private communication, 1984.

- [14] S. Friedland & R. Loewy, "Subspaces of Symmetric Matrices Containing Matrices with a Multiple First Eigenvalue," *Pacific J. Math.* 62 (1976), 389–399.
- [15] Y.-H. Au-Yeung & Y.-T. Poon, "A Remark on the Convexity and Positive Definiteness Concerning Hermitian matrices," *Southeast Asian Bull. Math.* 3 (1979), 85–92.
- [16] Y.-H. Au-Yeung & N.-K. Tsing, "An Extension of the Hausdorff-Toeplitz Theorem on the Numerical Range," *Proc. Amer. Math. Soc.* 89 (1983), 215–218.
- [17] M.K.H. Fan & A.L. Tits, "On the Generalized Numerical Range," *Linear and Multilinear Algebra* (1987), to appear.
- [18] F. Hausdorff, "Der Wertvorrat einer Bilinearform," *Math. Z.* 3 (1919), 314–316.
- [19] O. Toeplitz, "Das algebraische Analogon zu einem Satze von Fejér," *Math. Z.* 2 (1918), 187–197.
- [20] L. Brickman, "On the Field of Values of a Matrix," *Proc. Amer. Math. Soc.* 12 (1961), 61–66.
- [21] M. Marcus & C. Pesce, "Computer Generated Numerical Ranges and Some Resulting Theorems," *Linear and Multilinear Algebra* 20 (1987), 121–157.

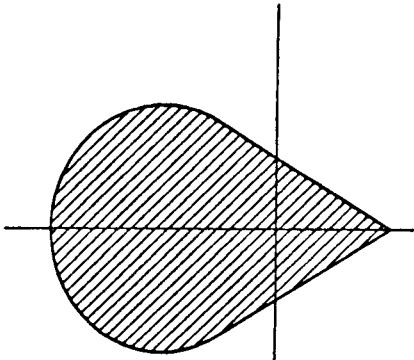


Fig. 1

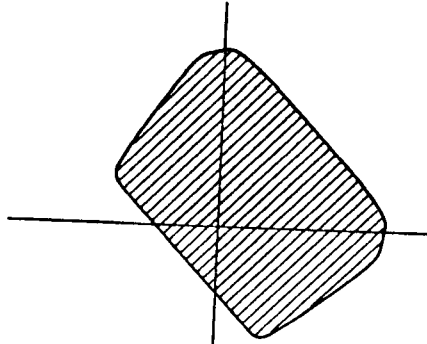


Fig. 2

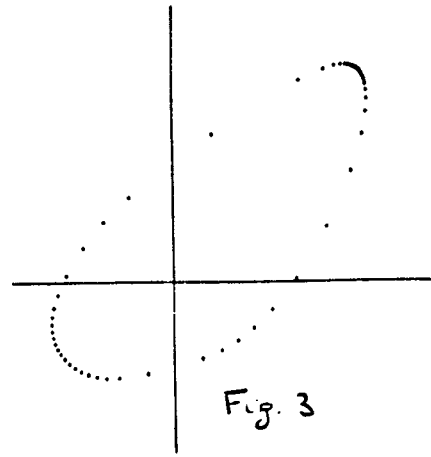


Fig. 3

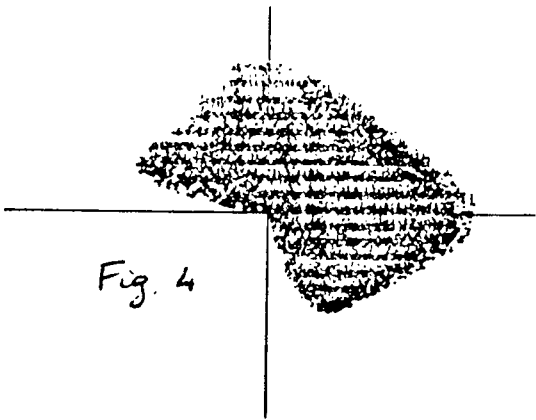


Fig. 4

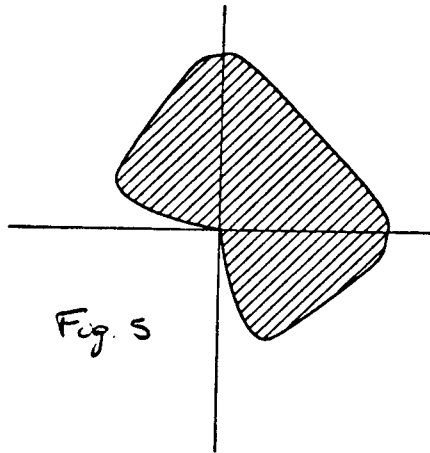


Fig. 5

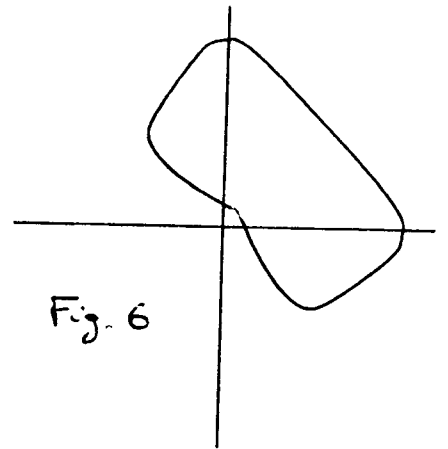


Fig. 6

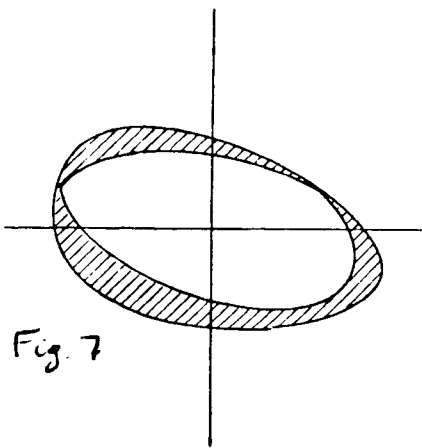


Fig. 7

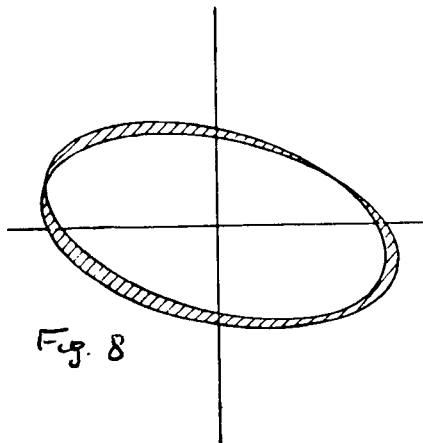


Fig. 8

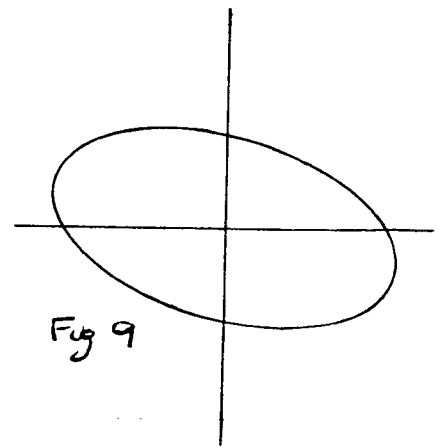


Fig. 9